Toxicogenomic Responses of the Model Organism *Caenorhabditis elegans* to Gold Nanoparticles

Olga V. Tsyusko,*[,†] Jason M. Unrine,[†] David Spurgeon,[§] Eric Blalock,[‖] Daniel Starnes,[†] Michael Tseng,[⊥] Greg Joice,[†] and Paul M. Bertsch[†,‡]

[†]Department of Plant and Soil Sciences, University of Kentucky, 1100 South Limestone Street, Lexington, Kentucky 40546, United States

[‡]Tracy Farmer Institute for Sustainability and the Environment, Lexington, Kentucky 40546, United States
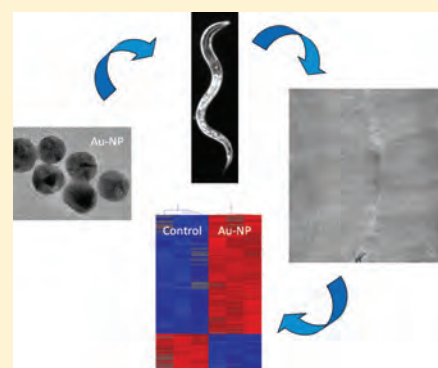
[§]Centre for Ecology & Hydrology, Maclean Building, Benson Lane, Crowmarsh Gifford, Wallingford, Oxforshire, OX10 8BB, United Kingdom

[‖]Department of Molecular and Biomedical Pharmacology, University of Kentucky, Lexington, Kentucky 40536, United States

[⊥]Department of Anatomical Sciences & Neurobiology, School of Medicine, University of Louisville, Louisville, Kentucky 40202, United States

ⓈSupporting Information

ABSTRACT: We used Au nanoparticles (Au-NPs) as a model for studying particle-specific effects of manufactured nanomaterials (MNMs) by examining the toxicogenomic responses in a model soil organism, *Caenorhabditis elegans*. Global genome expression for nematodes exposed to 4-nm citrate-coated Au-NPs at the LC_{10} level (5.9 mg·L^{-1}) revealed significant differential expression of 797 genes. The levels of expression for five genes (*apl-1*, *dyn-1*, *act-5*, *abu-11*, and *hsp-4*) were confirmed independently with qRT-PCR. Seven common biological pathways associated with 38 of these genes were identified. Up-regulation of 26 *pqn/abu* genes from noncanonical unfolded protein response (UPR) pathway and molecular chaperones (*hsp-16.1*, *hsp-70*, *hsp-3*, and *hsp-4*) were observed and are likely indicative of endoplasmic reticulum stress. Significant increase in sensitivity to Au-NPs in a mutant from noncanonical UPR (*pqn-5*) suggests possible involvement of the genes from this pathway in a protective mechanism against Au-NPs. Significant responses to Au-NPs in endocytosis mutants (*chc-1* and *rme-2*) provide evidence for endocytosis pathway being induced by Au-NPs. These results demonstrate that Au-NPs are bioavailable and cause adverse effects to *C. elegans* by activating both general and specific biological pathways. The experiments with mutants further support involvement of several of these pathways in Au-NP toxicity and/or detoxification.

INTRODUCTION

Due to the increasing number of consumer and industrial products containing manufactured nanomaterials (MNMs), there is growing concern about environmental releases and the subsequent potential impacts to both humans and ecoreceptors. The most common MNMs are composed of metal and metal oxides (www.nanoproject.org). Although a number of recent studies have investigated the ecotoxicity of metal and metal oxide nanoparticles, it can be difficult to differentiate between particle-specific effects and effects due to the release of free metal ions.[1−3] Gold nanoparticles (Au-NPs) have been used in previous studies as a particle-specific probe since they are resistant to oxidative dissolution.[3,4] Au-NPs are mainly being used for medical and imaging applications including sensing, gene and drug delivery, cell labeling, and as anti-HIV (human immunodeficiency virus) agents.[5−8] In our previous study using microfocused X-ray absorption spectroscopy, we demonstrated that *Caenorhabditis elegans* exposed to Au-NPs absorb Au as intact particles.[2] More recently we also presented multiple lines

of evidence for uptake and distribution of intact Au-NPs in earthworms, plants, and insect larvae.[3,4,9]

Recent multimedia fate modeling-based risk analyses have suggested that the majority of several classes of MNMs are expected to enter wastewater streams and in wastewater treatment plants partition to solid components, which are often applied to agricultural land as biosolids.[10] Studying the effects of Au-NPs on model organisms, such as the nematode *C. elegans*, which also serves as a model organism for ecotoxicity testing,[11−16] may provide additional insights into the environmental effects of MNMs, as has been possible previously for some conventional chemicals[17] and environmental disturbances,[16,18] including exposure to heavy metals.[19] Furthermore, because the complete sequenced genome of *C. elegans* is

known, whole genome microarrays are available, and various functional genetic tools (including RNAi and mutants) have been optimized, *C. elegans* provides an ideal soil invertebrate through which to study the toxicogenomic effects of Au-NP exposure. This will also provide a basis for future studies on the effects of environmental transformations of MNM on mechanisms of toxicity in soil organisms by identifying particle-specific responses. The toxicogenomic approach has been applied previously to examine changes in global transcriptomic profiles in *C. elegans* exposed to metals[20,21] and has been also extended to studies with Ag-NPs.[22]

Previous in vitro studies demonstrate conflicting results for Au-NP toxicity, with several showing a lack of toxicity,[23,24] while others demonstrated adverse effects related to the charge and size of the Au-NPs.[25,26] Several investigations have examined cellular processes and genes involved in toxicity of Au-NPs in vitro;[27,28] however, in vitro results by their nature cannot explain the full range of systemic toxicological effects that may influence the biology of a whole organism.[29] The majority of published in vivo studies on Au-NP toxicity (more than 12 studies are summarized in ref 30) have been conducted on mice and rats by using intravenous Au-NP injection.

The objective of this study was to examine the in vivo particle-specific toxicity of Au-NPs to *C. elegans* via the toxicogenomic approach. Differentially expressed genes identified from whole genome microarray analyses were linked to potential biological pathways involved in the toxicity of Au-NPs based on current annotation. To explore possible mechanisms of defense against toxicity of Au-NPs, gene expression inhibition experiments with RNA interference (RNAi) and with mutants were conducted for selected genes associated with pathways identified by microarray analyses to examine the phenotypic consequences of gene knockdown.

■ MATERIALS AND METHODS

Gold Nanoparticle Synthesis and Characterization. Stable aqueous suspensions of Au spheres with a nominal diameter of 4 nm were prepared by the citrate reduction method with 99.99% $HAuCl_4$ and >99% sodium citrate (Sigma−Aldrich, St. Louis, MO).[31] Primary particle size was measured by TEM (transmission electron microscopy; Hitachi H-8000, Pleasanton, CA), while particle hydrodynamic diameter in suspensions of exposure media was determined via dynamic light scattering (DLS) (Malvern Zetasizer nano ZS, Worcestershire, U.K.). Inductively coupled plasma mass spectrometry (ICP-MS) (Agilent 7500cx, Santa Clara, CA) was used to determine total Au concentrations in stock suspensions after dissolution in aqua regia and concentrations of dissolved Au after ultrafiltration with 3 kDa (0.9 nm pore size) ultrafiltration membranes (Amicon, Millipore, Billerica, MA). TEM images and DLS particle size distributions, including DLS data in actual exposure media, are given in Supporting Information (Figures S1 and S2).

Transmission Electron Microscopy and Energy-Dispersive Spectroscopy. These methods are presented in Supporting Information.

Nematode Exposures and Microarrays. Wild-type N2 strain of *C. elegans*, obtained from Caenorhabditis Genetics Center (CGC), were age-synchronized with the eggs placed on K-agar plates containing *Escherichia coli* OP50 as a food source.[32] The nematodes at L3 stage were exposed to five concentrations of Au-NPs (0, 2.5, 5.5, 7, 15, and 30 mg·L^{-1}) in 50% K-medium (31.68 mM KCl and 51.37 mM NaCl). At 12

h, all solutions were replaced with 50% K-medium and left for another 12 h. This exposure regime was selected because this study is a part of a larger-scale experiment investigating interactions between metals and nanoparticles. Results on the interactions will be presented in a future paper. All exposures were performed in 24-well tissue culture plates with 1 mL of exposure solution and 10 nematodes per well, with six replicates per concentration. Mortality was scored after 24 h. The concentration resulting in 10% mortality (LC_{10}) was determined to be 5.9 mg·L^{-1}, and this exposure concentration was used for the microarray experiment. Age-synchronized L3 nematodes (about 2000 nematodes per replicate, with three replicates per treatment) were exposed to LC_{10} in 6 cm Petri dishes with 4 mL of exposure solution per dish. After 24 h (with the exposure scenario being the same as for the mortality experiment), RNA was extracted from each of the replicates by use of Trizol (Invitrogen) followed by purification with Qiagen RNeasy Kit (Qiagen, Chatsworth, CA). Repeated freeze−thaw cycles (at −80 and 37 °C) were used to lyse the cells. All RNA samples were run on a Nanodrop ND-1000 spectrophotometer and bioanalyzer (Agilent) to quantify and check for RNA quality. All samples showed no signs of degradation with RINs (RNA integrity number) of 9 and 10. The RNA was sent to the microarray core facility at the University of Kentucky for processing via Affymetrix *C. elegans* whole genome microarrays. Biotin-labeled cRNA probes were prepared from 1 μg of total RNA, hybridized to the microarray chips for 16 h, washed to remove unhybridized cRNA by use of a fluidics station, and stained according to the standard GeneChip expression analysis technical manual. Chip scanning was conducted on the Affymetrix GCS 3000 7G scanner.

Raw expression data were normalized by use of the robust multiarray average (RMA) algorithm[33] followed by quantile normalization implemented in Partek Genomics Suite 6.4 (Partek, Inc., St Louis, MO). Hierarchical clustering was performed in Partek to confirm that the samples match to the treatment groups. Analysis of variance (ANOVA) was used to partition the variance due to treatment from technical and biological noise. The list of differentially expressed genes was generated by identifying the genes showing *x*-fold change of more than 1.5 and less than −1.5 at $p < 0.05$ with and without multiple sample correction, false discovery rate (FDR). False discovery correction according to Benjamini and Hochberg[34] produced a list of 37 significant transcripts. FDR was not applied when differentially expressed genes were selected, because this approach can increase the type II error and result in elimination of the genes responsive to the treatment.[17] All microarray data have been submitted to National Center for Biotechnology Information (NCBI) (accession number GSE32521). The gene list consisting of 797 genes (based on the uncorrected list) was imported into IPA (Ingenuity Systems, www.ingenuity.com) for analysis of biological functions linked to these genes and to study biologically relevant canonical pathways involving these genes. The same gene list was also used as input for the bioinformatics resource DAVID.[35] We used the functional annotation clustering tool in DAVID to identify significant changes within the gene list enriched annotation categories, such as GO terms, protein−protein interactions, and KEGG (Kyoto Encyclopedia of Genes and Genomes) biological pathways. Meta-analysis for comparison with four other microarray data sets deposited in GEO database was performed similarly as described by Blalock et al.[36] For comparison, we selected studies under different stress

4116

dx.doi.org/10.1021/es2033108 | *Environ. Sci. Technol.* 2012, 46, 4115−4124

conditions including exposure to Ag-NPs,[22] oxidative stress,[37] exposure to *Staphylococcus aureus*,[38] and *octr-1* mutant with resistance to *Pseudomonas aeruginosa*.[39] Details of the analysis are presented in Supporting Information. We also calculated representation factors (RF; Table 1) demonstrating whether genes from one data set are enriched in another data set.[40] The common genes were divided in four categories based on the direction of their response (Figure S7, Supporting Information), and significance of the response for each direction was inferred from χ^2 distribution.

Quantitative Reverse Transcription Polymerase Chain Reaction: Validation of Microarray Data. qRT-PCR analyses were conducted on samples from control and Au-NP-exposed nematodes. Three genes linked to two pathways identified by IPA (amyloid processing and endocytosis) were used for qRT-PCR: *apl-1* (amyloid precursor-like protein), *dyn-1* (dynamin), and *act-5* (actin). In addition, *hsp-4* (heat shock protein) and *abu-11* (activated in blocked unfolded protein response) were identified as differentially expressed genes involved respectively in canonical and noncanonical unfolded protein response (UPR). Glucose-6-phosphate isomerase I (*gpi-1*) was quantified as a reference gene, which did not show any significant changes within the microarray data and also after qRT-PCR confirmation. A total of 500 ng of RNA was used for conversion into cDNA with RNA-to-cDNA master mix (Applied Biosystems). The qRT-PCR was performed in a 10 μL reaction with 1× FastStart universal probe Roche master mix, 250 nM probe from Roche universal probe library, 900 nM of both primers, and 2 μL of diluted 1:18 cDNA. The list of primers and probes with their corresponding efficiencies (96−101%) is given in Table S1 in Supporting Information. All probes used spanned introns to avoid amplification of genomic DNA. TaqMan assays resulted in higher efficiencies for two genes, *gpi-1* and *act-5*, and were used for these genes. Amplification for all genes was performed by use of StepOne Plus system (Applied Biosystems) for 10 min at 95 °C, followed by 40 temperature cycles for 10 s at 95 °C and 30 s at 60 °C. All samples for every gene were run in triplicate. Negatives and minus reverse transcription (−RT) negatives were run for every gene/sample to check for DNA contamination. The data were exported into GenEx software (MultiD), and after normalization against the reference gene, *gpi-1*, the expression levels were calculated relative to controls following Pfaffl et al.[41]

To test whether unbound citrate had an effect on gene expression, we also exposed *C. elegans* to the suspensions that had particles removed by ultrafiltration. Au-NPs were filtered through 3 kDa cutoff regenerated cellulose centrifugal ultrafiltration devices, as described in the characterization section. Using nematodes exposed to the filtrates, we conducted qRT-PCR on a gene selected from citrate cycle pathway, ATP citrate-lyase (*D1005.1*), and two genes, *abu-11* and *dyn-1*, from pathways not related to citrate metabolism. The expression patterns were compared between the filtered and unfiltered Au-NPs and controls.

Inhibition of Gene Function by Use of Interference RNA and Toxicity Testing with Mutants. These methods are presented in Supporting Information. qRT-PCR was performed to confirm inhibition in the expression levels of the two genes *abu-11* and *dyn-1* after use of corresponding double-stranded RNAi (Figure S6, Supporting Information).

RESULTS AND DISCUSSION

The nematodes showed an increase in mortality with increasing Au-NP concentration (Figure 1). The LC_{10} of 5.9 mg·L^{-1} Au-
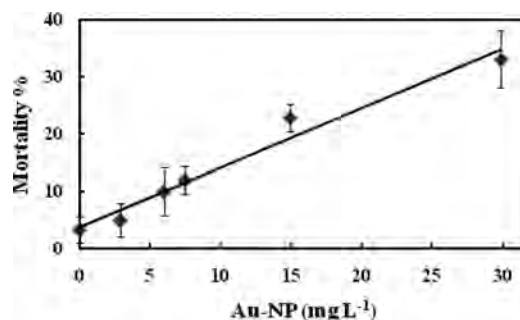

Figure 1. Mortality of *C. elegans* after exposure to citrate-coated 4 nm Au-NPs.

NPs that could be calculated from this response was used for microarray experiments. The Au fraction measured by ultrafiltration in the exposure solution after 24 h was (1.4×10^{-5})% of the maximum exposure concentration, indicating that the nanoparticles were not undergoing oxidative dissolution. After examining the entire length of *C. elegans* in multiple samples via TEM, consistent electron-dense particles were observed in the nematode's gut lumen and in microvilli (Figure S3, Supporting Information), but they were not found near the cuticle surface or penetrating the cuticle. The elemental composition of these particles was confirmed to be Au via energy-dispersive spectroscopy (EDS) analysis (Figure S4, Supporting Information). The presence of Au-NPs in the intestine and the inability to detect them near cuticle suggests that Au-NPs are being ingested and absorbed from the intestine. In our earlier study using microfocused synchrotron based X-ray absorption spectroscopy, we also suggested that *C. elegans* exposed to Au-NPs absorb Au as intact particles.[2] Other studies on Ag-NPs in nematodes[42] and Au-NPs in earthworms[43] have demonstrated that nanoparticles are absorbed and distributed intracellularly. Absence of evidence for Au-NP dissolution, coupled with the current and previous results, suggests that gene expression changes represent a response to Au-NPs, some of which may be internalized within cells.

Biological Pathways and Gene Ontology Categories Identified from Microarray Analysis. There were a total of 797 differentially expressed genes meeting the selection criteria, with a majority of the genes (542 genes) being up-regulated. A treatment-independent clustering histogram based on 797 genes reveals that the control and exposed replicates are grouped within respective clusters, clearly demonstrating the response of *C. elegans* to Au-NPs (Figure S5, Supporting Information). Data analysis using the IPA revealed five biological pathways that were significantly overrepresented in the differentially expressed gene list (Tables S2 and S3, Supporting Information) following Au-NP exposure: amyloid processing, citrate cycle, clathrin-mediated endocytosis, apoptosis, and G-protein signaling. Analyses of the same 797-gene list via DAVID identified the citrate cycle and two additional KEGG pathways [calcium signaling and mitogen-activated protein kinase (MAPK); Table S2, Supporting Information] that were significantly overrepresented in the gene list. Several differentially expressed genes were associated with two or three pathways (Table S3, Supporting Information). The list of the

Table 1. Representation Factors for Comparison of the Au-NP Data Set with Four Other Microarray Data Sets in Which *C. elegans* Are Exposed to a Variety of Stressors

		no. of significant genes[a]				
data set	no. of genes detected[b]	Au-NP study	other data set	common to both[c]	RF[d]	*P*-value[e]
Ag-NPs	9083	725	1621	187	1.45	6.6×10^{-7}
oxidative stress	9208	669	826	61	1.02	0.416
Staphylococcus aureus	7728	581	272	24	1.17	0.183
octr-1 exposed to *Pseudomonas aeruginosa*	10 299	731	3631	264	1.02	0.331

[a]Based on $p < 0.05$ and 1.5-fold change. [b]Number of genes rated present both in the current study and in the data set of interest. [c]Genes found to have changed significantly in both studies. [d]Representation factor (RF) = number of genes common to both studies divided by number of genes expected to be common in both studies. [e]Probability that such an overlapping number of genes could not occur by chance (from binomial test).

pathways identified through IPA and DAVID and differentially expressed genes from these pathways are listed in Tables S2 and S3 (Supporting Information).

Focusing on the 542 up-regulated genes at a threshold of 4 and $p < 0.05$, 165 significant biological process (BP), 46 cellular component (CC), and 32 molecular function (MF) gene ontology (GO) terms were identified. Many GO categories were represented by the same genes. To avoid redundancy, the functional annotation clustering tool in DAVID[35] was used by choosing the "GOTERM_BP_ALL", "GOTERM_CC_ALL", and "GOTERM_MF_ALL" options. Tables S4–S6 (Supporting Information) shows 25 BP, 12 CC, and 11 MF significant GOs, which were represented by the largest number of genes within each of these functional clusters. Among these GO categories for biological processes (Table S4, Supporting Information) are such large categories as developmental processes (GO:0032502), postembryonic development (GO:0009791), reproductive developmental processes (GO:0003006), regulation of growth (GO:0040008), cellular component organization (GO:0016043), and locomotion (GO:0040011). The GO analysis also identified smaller, more specific categories with some of them containing genes linked to the identified pathways. Among these GOs were endocytosis (GO:0006897), cellular response to unfolded proteins (GO:0034620), and aging (GO:0007568). Among GOs in the cellular component terms (Table S5, Supporting Information) are such categories as intracellular (GO:0005622), intracellular organelle part (GO:0044446), cytoplasmic part (GO:0044444), nuclear part (GO:0044428), and extracellular region (GO:0005576). Smaller categories that are associated with some of the identified pathways include cytoplasmic vesicle (GO:0031410) and actin cytoskeleton (GO:0015629). For GOs in molecular function terms (Table S6, Supporting Information), the most prominent ones are protein binding (GO:0005515), nucleotide binding (GO:0000166), ATP binding (GO:0005524), and enzyme regulator activity (GO:0030234).

Previous results on transcriptomic effects of Au-NPs are available from in vivo studies in mice where Au-NPs were administered by single injection intravenously and where liver and spleen were used for analyses.[30,44] Despite the differences between studies in exposure pathways (intravenous versus ingestion/dermal) and duration of the exposure (single dose versus continuous), there is some commonality in responses of *C. elegans* and mice to Au-NPs. For instance, Cho et al.[44] demonstrated that gene categories associated with apoptosis, cell cycle, signal transduction, metabolic process, vesicle-mediated transport, and response to stress were affected by poly(ethylene glycol)- (PEG-) coated Au-NPs. In *C. elegans*, one of the pathways detected by IPA is apoptosis, and among

the significant GO categories are GO:0007049, cell cycle; GO:0051246, regulation of protein metabolic process; and GO:0031410, cytoplasmic vesicle (Tables S2–S6, Supporting Information). Up-regulation of molecular chaperones, activation of noncanonical unfolded protein response (as discussed below), and genes related to necrosis can be also considered as indication of response to stress. Another study on Au-NP toxicity in rats[30] emphasized the significance of genes related to cell cycle, defense response, detoxification, lipid metabolism, and circadian rhythm. Interestingly, as well as cell cycle and stress responses, two *C. elegans* genes (*lin-42* and *tim-1*) homologous to *Drosophila* circadian clock genes and critical for timing of development[45] were significantly up-regulated in response to Au-NPs. Thus, our results and those of other in vivo studies hint at conserved transcriptomic responses to Au-NPs in this species.

Comparisons with Other Microarray Data Sets. Comparison analysis with four other data sets (Ag-NPs,[22] oxidative stress,[37] exposure to pathogen *Staphylococcus aureus*,[38] and resistance to pathogens in *octr-1* mutant[39]) revealed interesting results. Representation factors and *p*-values from the binomial tests suggest that only comparison with Ag-NPs resulted in significant outcome (Table 1; Figure S7, Supporting Information). The number of genes ($n = 187$) found in the overlap between Au-NP and Ag-NP is significantly higher than would be expected by chance alone ($p < 0.0001$), suggesting that there may be similarities in the genes that respond to Ag- and Au-NPs. However, more close analysis of the direction of the response of these genes reveals that there is a significantly higher number of genes ($n = 145$, $\chi^2 = 34.92$, $p < 0.001$) that responded in opposite directions, such as being up-regulated by Au-NPs but down-regulated by Ag-NPs and vice versa (Figure S7, Supporting Information). For instance, using DAVID we identified that the common genes up-regulated by Ag-NPs and down-regulated by Au-NPs belong to the molecular function GO category of metal ion binding (GO:0046872), further supporting that Au ions are not involved in Au-NP toxicity as they may be in Ag-NP toxicity. Analysis of common genes that are up-regulated by Au-NPs and down-regulated by Ag-NPs resulted in a longer list of GOs including such large categories in biological processes as locomotion, larval development, and reproduction. Among the molecular function terms are nucleotide binding, ATP binding, peptidase activity, and kinase activity. Overall, the meta-analysis of our study with the other four data sets indicates that exposure to Au-NPs resulted in rather unusual genetic signatures that do not show significant similarities when compared with the responses to other stress conditions analyzed.

Effect of Unbound Citrate on *C. elegans*. Before addressing in more detail the responses that are specific to Au-NP exposure, we address the question whether the presence of a small amount of unbound citrate alone could have an effect on the nematodes exposed to the citrate-coated Au-NPs. There were in total six genes related to the citrate cycle pathway identified by IPA and DAVID (Table S3, Supporting Information). Differential expression of one of these genes, ATP citrate-lyase (*D1005.1*), was independently confirmed by qRT-PCR. *C. elegans* exposed to filtrate obtained after centrifugation of Au-NPs through 3 kDa filters showed levels of expression of citrate-lyase similar to the levels observed in organism exposed to Au-NPs (Figure 2), suggesting that the
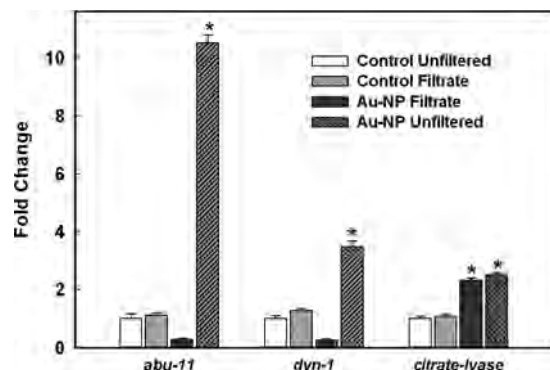
addition, the expressions of GTPase dynamin (*dyn-1*) and actin (*act-5*) were confirmed independently with qRT-PCR (Figure 3). Dynamin is involved in the early stages of endocytosis
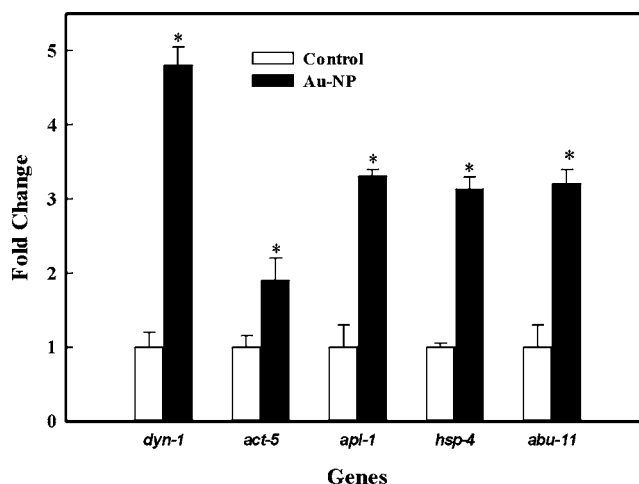

Figure 3. Independent qRT-PCR confirmation of expression levels for five genes in *C. elegans* exposed to 4 nm Au-NPs. Significant differences from control (asterisks) are shown at $p < 0.05$. Gene expression values were normalized to expression of *gpi-1* and shown as *x*-fold change relative to control.

Figure 2. Gene expression for three genes (*abu-11*, *dyn-1*, and citrate-lyase 1) for *C. elegans*, control and exposed to 5.9 mg·L^{-1}Au-NP solutions, unfiltered and filtered through 3 kDa membrane. The significant differences ($p < 0.05$) from control and Au-NP filtrates are shown by asterisks for *abu-11* and *dyn-1*. For citrate-lyase, the expression levels induced by filtered and unfiltered Au-NP suspensions are not different from each other but both are significantly different from controls. Gene expression values were normalized to expression of *gpi-1* and are shown as *x*-fold change relative to unfiltered control.

citrate may be inducing the genes related to the citrate cycle pathway. The question also arises whether the unbound citrate alone could have activated genes involved in other pathways. After nematodes were exposed to the same filtrate of Au-NPs, no up-regulation of *dyn-1* and *abu-11* (genes involved in endocytosis and unfolded protein response) was observed (Figure 2), confirming that the genes linked to pathways unrelated to citrate metabolism are not induced by free citrate in Au-NP suspensions.

Biological Pathways Affected by Gold Nanoparticles. *Endocytosis.* There were seven up-regulated genes (*act-5*, *apb-1*, *chc-1*, *dyn-1*, *hsp-1*, *rab-11.1*, and *wsp-1*) identified by IPA that have been implicated in clathrin-mediated endocytosis. Endocytosis is a process of transporting extracellular cargo from plasma membrane to the inside of the cell through vesicular transport.[46] During clathrin-mediated endocytosis, an invaginated clathrin-coated vesicle is formed, which is then pinched off the plasma membrane and carried to early endosome. The fate of cargo within this vesicle is determined in the early endosome, where it can be recycled back to the cell membrane or can be moved to late endosomes and eventually to lysosomes for degradation. We observed up-regulation of the genes that are responsible for recognition of cargo proteins (adaptin, *apb-1*), for forming clathrin coating (clathrin heavy chain, *chc-1*), and for mediating the recycle process of cargo from the early endosome (*rab-11.1*). In

during vesicle formation by promoting membrane fission of clathrin-coated vesicles from plasma membrane.[47] There is also another function of *dyn-1* associated with apoptosis and phagocytosis that is discussed below. *Act-5*, expression of which is limited to intestinal tissue, is essential for microvilli formation.[48] Another gene, *eps-8*, which is associated with microvilli tips and linked to endocytosis,[49] was also up-regulated in response to Au-NP exposure. Up-regulation of these two "microvilli" genes is likely to be induced by the presence of Au-NP in the intestine and microvilli, as shown by TEM and EDS in Figures S3 and S4 (Supporting Information). Given the up-regulation of multiple genes involved in the endocytosis pathway, it is likely that clathrin-dependent endocytosis is the primary process by which 4 nm citrate-capped Au-NPs are taken up into the cells, as has been previously suggested.[50] Our experiments performed with endocytosis mutants (*dyn-1*, *chc-1*, and *rme-2*) demonstrated no differences in *dyn-1* (results are not shown), significantly higher sensitivity of *chc-1*, and lower mortality in *rme-2* mutants exposed to Au-NPs in comparison with wild-type N2 nematodes (Figure 4). Significant response to Au-NP exposure in two out of the three tested mutants confirms that endocytosis is an important pathway for toxicity and detoxification of Au-NPs. Further studies with imaging of Au-NP distribution in endocytosis pathway-deficient *C. elegans* mutants may help explain the differences in responses of these endocytosis mutants.

Amyloid Processing Pathway. There was a total of six up-regulated *C. elegans* genes (*apl-1*, *clp-1*, *kin-19*, *par-1*, *kin-1*, and *kin-2*) homologous to genes associated with the human amyloid processing pathway.[51] The up-regulation of *apl-1*, amyloid precursor-like protein, which is homologous to human amyloid precursor protein (*app-1*) associated with Alzheimer's disease,[52] was independently confirmed with qRT-PCR (Figure 3). Changes in expression levels of human *app-1* are associated with the accumulation of β-amyloids, which triggers a cascade
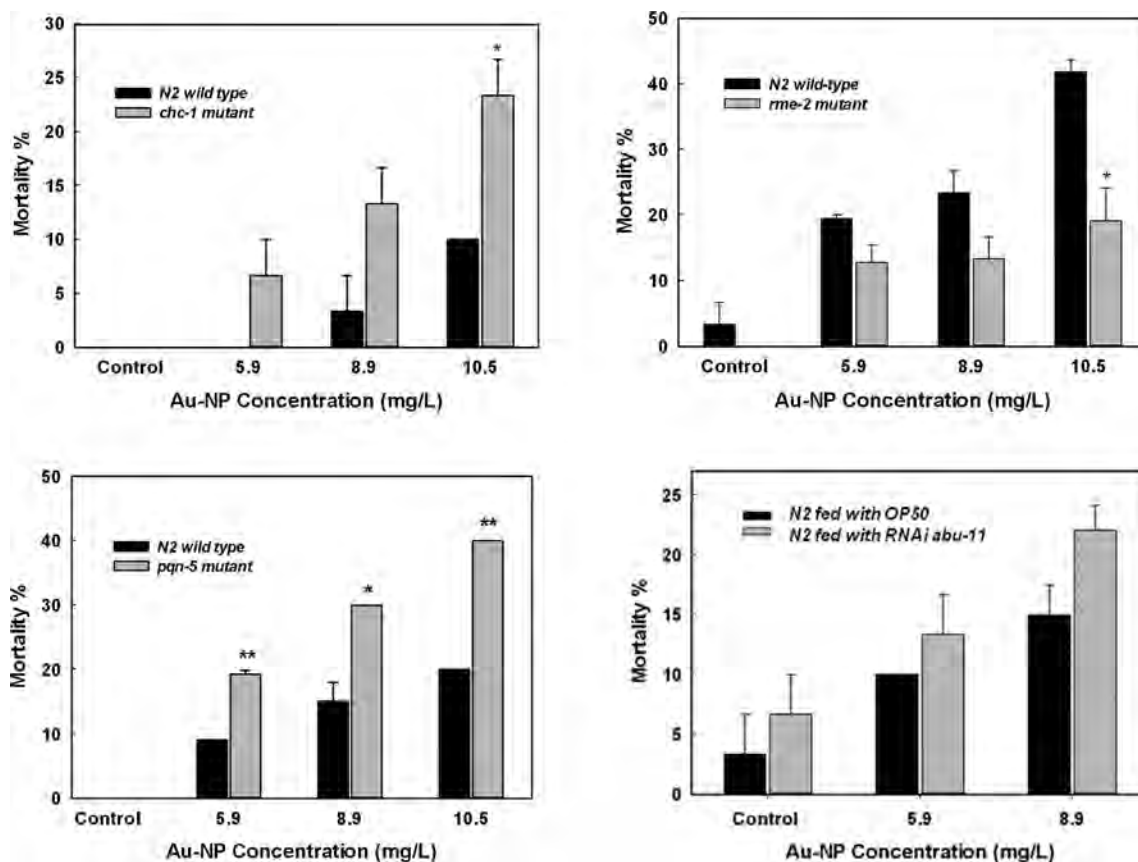
Figure 4. Mortality of *C. elegans* for wild type, mutants (*chc-1*, *rme-2*, and *pqn-5*), and N2s with *abu-11* inhibited by RNAi after exposure to Au-NPs. The significance levels are indicated by **$p < 0.01$ and *$0.01 < p < 0.05$.

of events including destabilization of intracellular calcium levels regulated by calpain (*clp-1* in *C. elegans*), eventually leading to neuronal degeneration.[51] In *C. elegans*, *apl-1* is expressed in multiple tissues, being important for molting, morphogenesis, and larval survival.[53] Together with *feh-1* (homologue of mammalian Fe65), which is expressed in neuromuscular structures of the pharynx and which was also up-regulated in response to Au-NPs, *apl-1* forms a complex controlling the rate of pharyngeal pumping.[54] Even though *C. elegans* does not accumulate β-amyloids, activation of genes homologous to those in the amyloid processing pathway may be indicative of events leading to neurodegeneration and can be also a result of unfolded protein response (described below) activated in response to Au-NP exposure.

Unfolded Protein Response. Ingenuity pathway analysis is specific to the human–mouse database, and as a result, 415 significantly up- and down-regulated genes were excluded from the IPA pathway analysis. From this population, we identified a group of 26 up-regulated genes from the *pqn* family with *x*-fold changes ranging from 1.5 to 8. These genes were also identified with DAVID in GO cellular component in protein binding (GO:0005515) category, and they encode proteins with prion-like glutamine/asparagines (Q/N)-rich domains.[55] These genes have been shown to be activated in noncanonical unfolded protein response (UPR) to endoplasmic reticulum (ER) stress.[55] Eleven genes in the *pqn* family are called *abu* (activated in blocked unfolded protein response) genes because they were shown to be up-regulated by exposure to tunicamycin (inducer of ER stress) in mutants (*xbp-1*) where canonical UPR response is blocked.[55] There were seven *abu* genes and 18 *pqn*

(Table S7, Supporting Information) genes that were significantly induced by exposure to Au-NPs. The *abu/pqn* genes have been shown to be transcriptionally controlled by apoptotic receptor, *ced-1*, and are involved in immune defense mechanism of *C. elegans* to pathogens.[56] Sun et al.[39] have demonstrated that sensory neurons (ASH and ASI) negatively regulate expression of the *pqn/abu* genes to suppress innate immune response to pathogens. The other *C. elegans* sensory neurons (AQR, PQR, and URX) have been shown to regulate activation of the mitogen-activated protein kinase (MAPK) pathway in response to pathogens.[57] MAPK was also one of the pathways identified by DAVID activated in response to Au-NPs. There were five up-regulated genes from this pathway (*hsp-1*, *lit-1*, *mnk-1*, *nsy-1*, and *lin-1*; Table S3, Supporting Information). Induction of the two pathways, MAPK and noncanonical UPR, regulated by sensory neurons may be suggestive of involvement of sensory neurons in regulating responses to stress caused by Au-NPs, similarly to how responses to pathogens are regulated. The totality of responses to Au-NPs, however, differed from responses to model pathogens, as revealed by low RF in our meta-analysis (Table 1).

Activation of MAPK and UPR may be also linked to the response to the accumulation of unfolded and aberrant proteins caused by Au-NP exposure. Endoplasmic reticulum stress is characterized by accumulation of unfolded/misfolded proteins and alteration in Ca^{2+} homeostasis. It has been previously hypothesized that Au-NPs may cause denaturation and misfolding of proteins.[50] Several specific signaling pathways, which reside in a complex referred to as canonical UPR, are activated in response to ER stress to assist with correct protein

4120

dx.doi.org/10.1021/es2033108 | *Environ. Sci. Technol.* 2012, 46, 4115–4124

folding by activating molecular chaperones, degradation of misfolded proteins, and overall decrease in protein synthesis.[58] Up-regulation of the molecular chaperones *hsp-3*, *hsp-4*, *hsp-70*, and *hsp-16.1* was also observed in response to Au-NPs, which is indicative of the chaperoning response to unfolded proteins and, hence, ER stress. Up-regulation of *hsp-4*, a marker of ER stress,[55] was confirmed independently with qRT-PCR (Figure 3).

Two of the genes from noncanonical UPR (*abu-11* and *pqn-5*), the overexpression of which has been shown to increase nematode life span[59] and which have been upregulated by Au-NPs (at 2.7- and 8.5-fold change, respectively, from microarray results) were selected for further experiments with inhibition of gene function with RNAi (*abu-11*) and a mutant strain (*pqn-5*). Our hypothesis was that inhibition of function with RNAi or its impairment in the mutant would increase sensitivity to Au-NPs since molecular chaperone functions would be restricted. When *abu-11* function was inhibited, exposure to 8.9 mg·L^{-1} Au-NP showed a trend toward increased mortality from 15% to 21% (p = 0.068) (Figure 4). The *pqn-5* mutants demonstrated significantly higher sensitivity to Au-NP exposure at all tested concentrations (Figure 4), thus confirming our previous hypothesis. Nine of the *pqn/abu* genes, including *abu-11* and *pqn-5*, are located together on mountain 29 of the *C. elegans* topographical expression map,[40] and their activity is likely to be coregulated.[56] It is possible that function of more than one of the *abu* genes would need to be inhibited in order to show a more significant increase in sensitivity to Au-NP exposure for *abu-11*. In addition, other chaperonin pathways may be compensating for the inhibition of *abu-11*.

Necrosis and Apoptosis. ER stress can also result in apoptosis and/or necrosis of cells with accumulated misfolded proteins. It has been suggested that a common set of genes is involved in elimination of cell corpses through two different mechanisms of cell death, apoptosis and necrosis.[60] Most apoptotic events occur in *C. elegans* during development and the fixed number of cells in adults are not expected to undergo programmed cell death after development;[61] therefore, apoptotic events are likely to occur in the germline. It appears that exposure to Au-NPs, if not resolved through activation of UPR, may result in apoptosis and/or necrosis. Apoptosis was one of the pathways induced by the Au-NPs identified via DAVID. This was based on up-regulation of five genes (*cogc-5*, *clp-1*, *ced-3*, *pme-1*, and *spc-1*; Table S3, Supporting Information). In addition, several of the pathways activated in *C. elegans* exposed to Au-NPs are involved in conserved mechanism for necrosis (the so-called calpain–cathepsin hypothesis).[62] According to this mechanism, destabilization of Ca^{2+} channels results in increased intracellular Ca^{2+} concentrations. In response to the elevated Ca^{2+}, calpains become activated, affecting integrity of lysosome membranes and resulting in release of cathepsin proteases from the lysosome, which eventually leads to cell death.[62] Activation of Ca signaling pathway after exposure to Au-NPs (Tables S2 and S3, Supporting Information) involves up-regulation of G-proteins (*gsa-1* and *gpb-1*), which has been shown previously to increase the Ca^{2+} level inside cells and trigger necrosis.[63] Up-regulation of sarco/endoplasmic reticulum Ca^{2+} ATPase SERCA (*sca-1*) and calumenin (*calu-1*) in response to Au-NPs suggests that the exposed nematodes enhance calcium handling overall.[64] Up-regulation of calpains (*clp-1*, *clp-4*, and *clp-7*) is also observed in Au-NP-exposed nematodes. In the presence of this change in Ca trafficking, lysosome rupture and

release of lysosomal hydrolases into cytoplasm, as indicated by the presence of cathepsin L (*cpl-1*), can take place. Three genes (*ced-1*, *rab-7*, and *dyn-1*) involved in apoptosis/necrosis regulation were up-regulated in response to Au-NPs. The phagocytic receptor *ced-1* recognizes dying cells and initiates phagocytosis;[65] *rab-7* participates in lysome fusion with phagocytes; and *dyn-1*, a gene already discussed in relation to endocytosis, regulates delivery of vesicles to the phagocytic cups to contribute to pseudopod extension around necrotic cells.[66−68] Apoptotic/necrotic events observed in this study can also be related to the exposure concentration of 5.9 mg·L^{-1}, which caused 10% of nematode mortality. To investigate the function of the apoptosis/necrosis pathway in the Au-NP response, we examined whether an RNAi knockdown of *dyn-1* or *dyn-1* mutants would have increased sensitivity to Au-NPs, based on the hypothesis that inhibition of the *dyn-1* function may affect phagocytosis processes and result in accumulation of necrotic cells. RNAi and mutants did not, however, confirm this hypothesis since no differences in mortalities induced by Au-NPs were found between control and *dyn-1* RNAi-treated nematodes or *dyn-1* mutants (data not shown). It is possible that alternative genes or a combination of several necrosis-related pathways may be involved in response to Au-NP insult.

The results from this and previous studies provide evidence that intact citrate-coated 4 nm Au-NPs are bioavailable, can induce specific and more general biological pathways, and are capable of causing adverse effects on whole organisms. On the basis of gene expression profiles, we propose likely mechanisms that link Au-NP exposure to toxic effects in *C. elegans*. Activation of the endocytosis pathway suggests that Au-NPs can be taken inside the cell through clathrin-mediated endocytosis. While inside the cell, they cause ER stress, resulting in increased amounts of misfolded or unfolded proteins and activation of canonical (molecular chaperones) and noncanonical UPR pathways, specific to *C. elegans* and controlled by *abu/pqn* genes. Activation of UPR leads to survival of the cell or, in case of excess accumulation of misfolded proteins, to cell death. Au-NPs also seem to activate Ca signaling and amyloid processing pathways, which lead to intracellular Ca^{2+} increase and trigger calpain−cathepsin-mediated events leading to cell necrosis and ultimately to mortality. This study can serve as a starting point for future studies investigating what particle-specific properties affect toxicity of MNM in soil invertebrates, such as *C. elegans*, including the role of environmental transformations of MNM.

■ ASSOCIATED CONTENT

ⓢ Supporting Information

Additional text with methods for TEM and EDS, inhibition with RNAi, toxicity testing with mutants, and meta-analysis, and seven tables and seven figures as described in the text. This material is available free of charge via the Internet at http://pubs.acs.org.

■ AUTHOR INFORMATION

Corresponding Author
*E-mail: olga.tsyusko@uky.edu.

Notes

The authors declare no competing financial interest.

■ ACKNOWLEDGMENTS

■ REFERENCES

(1) Shoults-Wilson, W.; Reinsch, B.; Tsyusko, O.; Bertsch, P.; Lowry, G.; Unrine, J. Toxicity of silver nanoparticles to the earthworm (*Eisenia fetida*): The role of particle size and soil type. *Soil Sci. Soc. Am. J.* **2011**, *75*, 365−377.

(2) Unrine, J.; Bertsch, P.; Hunyadi, S. Bioavailability, trophic transfer, and toxicity of manufactured metal and metal oxide nanoparticles in terrestrial environments. In *Nanoscience and Nanotechnology: Environmental and Health Impacts*; Grassian, V., Ed.; John Wiley and Sons: Hoboken, NJ, 2008; pp 345−366.

(3) Unrine, J. M.; Hunyadi, S. E.; Tsyusko, O. V.; Rao, W.; Shoults-Wilson, W. A.; Bertsch, P. M. Evidence for bioavailability of Au nanoparticles from soil and biodistribution within earthworms (*Eisenia fetida*). *Environ. Sci. Technol.* **2010**, *44* (21), 8308−8313.

(4) Judy, J. D.; Unrine, J. M.; Bertsch, P. M. Evidence for biomagnification of gold nanoparticles within a terrestrial food chain. *Environ. Sci. Technol.* **2010**, *45* (2), 776−781.

(5) Chen, C. Y.; Xing, G. M.; Wang, J. X.; Zhao, Y. L.; Li, B.; Tang, J.; Jia, G.; Wang, T. C.; Sun, J.; Xing, L.; Yuan, H.; Gao, Y. X.; Meng, H.; Chen, Z.; Zhao, F.; Chai, Z. F.; Fang, X. H. Multihydroxylated [Gd@C$_{82}$(OH)$_{22}$]$_n$ nanoparticles: antineoplastic activity of high efficiency and low toxicity. *Nano Lett.* **2005**, *5* (10), 2050−2057.

(6) Di Gianvincenzo, P.; Marradi, M.; Martínez-Ávila, O. M.; Bedoya, L. M.; Alcamí, J.; Penadés, S. Gold nanoparticles capped with sulfate-ended ligands as anti-HIV agents. *Bioorg. Med. Chem. Lett.* **2010**, *20* (9), 2718−2721.

(7) Everts, M.; Saini, V.; Leddon, J. L.; Kok, R. J.; Stoff-Khalili, M.; Preuss, M. A.; Millican, C. L.; Perkins, G.; Brown, J. M.; Bagaria, H.; Nikles, D. E.; Johnson, D. T.; Zharov, V. P.; Curiel, D. T. Covalently linked au nanoparticles to a viral vector: Potential for combined photothermal and gene cancer therapy. *Nano Lett.* **2006**, *6* (4), 587−591.

(8) Gao, D.; Agayan, R. R.; Xu, H.; Philbert, M. A.; Kopelman, R. Nanoparticles for two-photon photodynamic therapy in living cells. *Nano Lett.* **2006**, *6* (11), 2383−2386.

(9) Sabo-Attwood, T.; Unrine, J. M.; Stone, J. W.; Murphy, C. J.; Ghoshroy, S.; Blom, D.; Bertsch, P. M.; Newman, L. A., Uptake, distribution and toxicity of gold nanoparticles in tobacco (*Nicotiana xanthi*) seedlings. *Nanotoxicology* [Online early access]. DOI: 10.3109/17435390.2011.579631. Published online: May 16, 2011.

(10) Gottschalk, F.; Sonderer, T.; Scholz, R. W.; Nowack, B. Modeled environmental concentrations of engineered nanomaterials (TiO$_2$, ZnO, Ag, CNT, fullerenes) for different regions. *Environ. Sci. Technol.* **2009**, *43* (24), 9216−9222.

(11) Boyd, W. A.; Williams, P. L. Comparison of the sensitivity of three nematode species to copper and their utility in aquatic and soil toxicity tests. *Environ. Toxicol. Chem.* **2003**, *22* (11), 2768−2774.

(12) Dhawan, R.; Dusenbery, D.; Williams, P. Comparison of lethality, reproduction, and behavior as toxicological endpoints in the nematode *Caenorhabditis elegans*. *J. Toxicol. Environ. Health* **1999**, *58*, 451−462.

(13) Leung, M. C. K.; Williams, P. L.; Benedetto, A.; Au, C.; Helmcke, K. J.; Aschner, M.; Meyer, J. N. *Caenorhabditis elegans*: an emerging model in biomedical and environmental toxicology. *Toxicol. Sci.* **2008**, *106*, 5−28.

(14) Dusenbery, D.; Williams, P. Aquatic toxicity testing using the nematode *Caenorhabditis elegans*. *Environ. Toxicol. Chem.* **1990**, *9*, 1285−1290.

(15) Freeman, M.; Peredney, C.; Williams, P., A soil bioassay using the nematode *Caenorhabditis elegans*. In *Environmental Toxicology and Risk Assessment: Standardization of Biomarkers for Endocrine Disruption and Environmental Assessment*; Henshel, D. S., Black, M. C., Harrass, M. C., Eds.; American Society for Testing and Materials: West Conshohocken, PA, 2000; pp 305−318.

(16) Höss, S.; Williams, P. L. Ecotoxicity testing with nematodes. In *Nematodes as Environmental Indicators*; Wilson, M. J., Kakaouli-Duarte, T., Eds.; CABI: Cambridge, MA, 2009; pp 208−224.

(17) Swain, S.; Wren, J. F.; Sturzenbaum, S. R.; Kille, P.; Morgan, A. J.; Jager, T.; Jonker, M. J.; Hankard, P. K.; Svendsen, C.; Owen, J.; Hedley, B. A.; Blaxter, M.; Spurgeon, D. J. Linking toxicant physiological mode of action with induced gene expression changes in *Caenorhabditis elegans*. *BMC Syst. Biol.* **2010**, *4*, 32.

(18) Bongers, T.; Ferris, H. Nematode community structure as a bioindicator in environmental monitoring. *Trends Ecol. Evol.* **1999**, *14* (6), 224−228.

(19) Roh, J.-Y.; Lee, J.; Choi, J. Assessment of stress-related gene expression in the heavy metal exposed nematode *Caenorhabditis elegans*: a potential biomarker for metal-induced toxicity monitoring and environmental risk assessment. *Environ. Toxicol. Chem.* **2006**, *25* (11), 2946−2956.

(20) Tominaga, N.; Matsuno, T.; Kohra, S.; Arizono, K., Sensing of heavy metals using *Caenorhabditis elegans* DNA microarray. In *Interdisciplinary Studies on Environmental Chemistry - Biological Responses to Chemical Pollutants*; Murakami, Y., Nakayama, K., Kitamura, S.-I., Iwata, H., Tanabe, S., Eds.; Terrapub: Tokyo, 2008.

(21) Cui, Y.; McBride, S. J.; Boyd, W. A.; Alper, S.; Freedman, J. H. Toxicogenomic analysis of *Caenorhabditis elegans* reveals novel genes and pathways involved in the resistance to cadmium toxicity. *Genome Biol.* **2007**, *8*, R122.

(22) Roh, J.-y.; Sim, S. J.; Yi, J.; Park, K.; Chung, K. H.; Ryu, D.-y.; Choi, J. Ecotoxicity of silver nanoparticles on the soil nematode *Caenorhabditis elegans* using functional ecotoxicogenomics. *Environ. Sci. Technol.* **2009**, *43* (10), 3933−3940.

(23) Connor, E. E.; Mwamuka, J.; Gole, A.; Murphy, C. J.; Wyatt, M. D. Gold nanoparticles are taken up by human cells but do not cause acute cytotoxicity. *Small* **2005**, *1* (3), 325−327.

(24) Shukla, R.; Bansal, V.; Chaudhary, M.; Basu, A.; Bhonde, R. R.; Sastry, M. Biocompatibility of gold nanoparticles and their endocytotic fate inside the cellular compartment: a microscopic overview. *Langmuir* **2005**, *21* (23), 10644−10654.

(25) Goodman, C. M.; McCusker, C. D.; Yilmaz, T.; Rotello, V. M. Toxicity of gold nanoparticles functionalized with cationic and anionic side chains. *Bioconjugate Chem.* **2004**, *15*, 897−900.

(26) Pan, Y.; Neuss, S.; Leifert, A.; Fischler, M.; Wen, F.; Simon, U.; Schmid, G.; Brandau, W.; Jahnen-Dechent, W. Size-dependent cytotoxicity of gold nanoparticles. *Small* **2007**, *3* (11), 1941−1949.

(27) Li, J. J.; Zou, L.; Hartono, D.; Ong, C. N.; Bay, B. H.; Lanry Yung, L. Y. Gold nanoparticles induce oxidative damage in lung fibroblasts in vitro. *Adv. Mater.* **2008**, *20* (1), 138−142.

(28) Schaeublin, N. M.; Braydich-Stolle, L. K.; Schrand, A. M.; Miller, J. M.; Hutchison, J.; Schlager, J. J.; Hussain, S. M. Surface charge of gold nanoparticles mediates mechanism of toxicity. *Nanoscale* **2011**, *3* (2), 410−420.

(29) Zhang, X. D.; Wu, H. Y.; Wu, D.; Wang, Y. Y.; Chang, J. H.; Zhai, Z. B.; Meng, A. M.; Liu, P. X.; Zhang, L. A.; Fan, F. Y.

Toxicologic effects of gold nanoparticles in vivo by different administration routes. *Int J Nanomed.* **2010**, *5*, 771−81.

(30) Balasubramanian, S. K.; Jittiwat, J.; Manikandan, J.; Ong, C.-N.; Yu, L. E.; Ong, W.-Y. Biodistribution of gold nanoparticles and gene expression changes in the liver and spleen after intravenous administration in rats. *Biomaterials* **2010**, *31* (8), 2034−2042.

(31) Jana, N. R.; Gearheart, L.; Murphy, C. J. Seeding growth for size control of 5−40 nm diameter gold nanoparticles. *Langmuir* **2001**, *17* (22), 6782−6786.

(32) Williams, P.; Dusenbery, D. Using the nematode *Caenorhabditis elegans* to predict mammalian acute lethality to metallic salts. *Toxicol. Ind. Health* **1988**, *4* (4), 469−478.

(33) Irizarry, R. A.; Hobbs, B.; Collin, F.; Beazer-Barclay, Y. D.; Antonellis, K. J.; Scherf, U.; Speed, T. P. Exploration, normalization, and summaries of high density oligonucleotide array probe level data. *Biostatistics* **2003**, *4* (2), 249−264.

(34) Benjamini, Y.; Hochberg, Y. Controlling the false discovery rate: a practical and powerful approach to multiple testing. . *J. R. Stat. Soc., Ser. B* **1995**, *57* (1), 289−300.

(35) Huang, D. W.; Sherman, B. T.; Lempicki, R. A. Systematic and integrative analysis of large gene lists using DAVID bioinformatics resources. *Nat. Protocols* **2009**, *4* (1), 44−57.

(36) Blalock, E. M.; Buechel, H. M.; Popovic, J.; Geddes, J. W.; Landfield, P. W. Microarray analyses of laser-captured hippocampus reveal distinct gray and white matter signatures associated with incipient Alzheimer's disease. *J. Chem. Neuroanat.* **2011**, *42* (2), 118−126.

(37) Park, S.-K.; Tedesco, P. M.; Johnson, T. E. Oxidative stress and longevity in *Caenorhabditis elegans* as mediated by SKN-1. *Aging Cell* **2009**, *8* (3), 258−269.

(38) Irazoqui, J. E.; Troemel, E. R.; Feinbaum, R. L.; Luhachack, L. G.; Cezairliyan, B. O.; Ausubel, F. M. Distinct pathogenesis and host sesponses during infection of *C. elegans* by *P. aeruginosa* and *S. aureus*. *PLoS Pathogen.* **2010**, *6* (7), e1000982.

(39) Sun, J.; Singh, V.; Kajino-Sakamoto, R.; Aballay, A. Neuronal GPCR controls innate immunity by regulating noncanonical unfolded protein response genes. *Science* **2011**, *332* (6030), 729−732.

(40) Kim, S. K.; Lund, J.; Kiraly, M.; Duke, K.; Jiang, M.; Stuart, J. M.; Eizinger, A.; Wylie, B. N.; Davidson, G. S. A gene expression map for *Caenorhabditis elegans*. *Science* **2001**, *293* (5537), 2087−2092.

(41) Pfaffl, M. W.; Horgan, G. W.; Dempfle, L. Relative expression software tool (REST (c)) for group-wise comparison and statistical analysis of relative expression results in real-time PCR. *Nucleic Acids Res.* **2002**, *30* (9), No. e36.

(42) Meyer, J. N.; Lord, C. A.; Yang, X. Y.; Turner, E. A.; Badireddy, A. R.; Marinakos, S. M.; Chilkoti, A.; Wiesner, M. R.; Auffan, M. Intracellular uptake and associated toxicity of silver nanoparticles in *Caenorhabditis elegans*. *Aquat. Toxicol.* **2010**, *100* (2), 140−150.

(43) Unrine, J. M.; Hunyadi, S. E.; Tsyusko, O. V.; Rao, W.; Shoults-Wilson, W. A.; Bertsch, P. M. Evidence for bioavailability of Au nanoparticles from soil and biodistribution within earthworms (*Eisenia fetida*). *Environ. Sci. Technol.* **2010**, *44* (21), 8308−8313.

(44) Cho, W. S.; Kim, S.; Han, B. S.; Son, W. C.; Jeong, J. Comparison of gene expression profiles in mice liver following intravenous injection of 4 and 100 nm-sized PEG-coated gold nanoparticles. *Toxicol. Lett.* **2009**, *191* (1), 96−102.

(45) Banerjee, D.; Kwok, A.; Lin, S.-Y.; Slack, F. J. Developmental timing in *C. elegans* is regulated by kin-20 and tim-1, homologs of core circadian clock genes. *Dev. Cell* **2005**, *8* (2), 287−295.

(46) Shivas, J. M.; Morrison, H. A.; Bilder, D.; Skop, A. R. Polarity and endocytosis: reciprocal regulation. *Trends Cell Biol.* **2010**, *20* (8), 445−452.

(47) Praefcke, G. J. K.; McMahon, H. T. The dynamin superfamily: universal membrane tubulation and fission molecules? *Nat. Rev. Mol. Cell Biol.* **2004**, *5* (2), 133−147.

(48) MacQueen, A. J.; Baggett, J. J.; Perumov, N.; Bauer, R. A.; Januszewski, T.; Schriefer, L. Waddle, J. A., ACT-5 is an essential *Caenorhabditis elegans* actin required for intestinal microvilli formation. *Mol. Biol. Cell* **2005**, *16* (7), 3247−3259.

(49) Kuwahara, T.; Koyama, A.; Koyama, S.; Yoshina, S.; Ren, C.-H.; Kato, T.; Mitani, S.; Iwatsubo, T. A systematic RNAi screen reveals involvement of endocytic pathway in neuronal dysfunction in *α*-synuclein transgenic *C. elegans*. *Hum. Mol. Genet.* **2008**, *17* (19), 2997−3009.

(50) Nel, A. E.; Mädler, L.; Velegol, D.; Xia, T.; Hoek, E.; Somarsundaran, P.; Klaessig, F.; Castranova, V.; Thompson, M. Understanding biophysicochemical interactions at the nano-bio interface. *Nat. Mater.* **2009**, *8*, 543−557.

(51) Selkoe, D. J. Alzheimer's disease: Genes, proteins, and therapy. *Physiol. Rev.* **2001**, *81* (2), 741−766.

(52) Zheng, H.; Koo, E. Biology and pathophysiology of the amyloid precursor protein. *Mol. Neurodegen.* **2011**, *6* (1), 27.

(53) Hornsten, A.; Lieberthal, J.; Fadia, S.; Malins, R.; Ha, L.; Xu, X.; Daigle, I.; Markowitz, M.; O'Connor, G.; Plasterk, R.; Li, C. APL-1, a *Caenorhabditis elegans* protein related to the human *β*-amyloid precursor protein, is essential for viability. *Proc. Natl. Acad. Sci. U.S.A.* **2007**, *104* (6), 1971−1976.

(54) Zambrano, N.; Bimonte, M.; Arbucci, S.; Gianni, D.; Russo, T.; Bazzicalupo, P. feh-1 and apl-1, the *Caenorhabditis elegans* orthologues of mammalian Fe65 and *β*-amyloid precursor protein genes, are involved in the same pathway that controls nematode pharyngeal pumping. *J. Cell Sci.* **2002**, *115* (7), 1411−1422.

(55) Urano, F.; Calfon, M.; Yoneda, T.; Yun, C.; Kiraly, M.; Clark, S. G.; Ron, D. A survival pathway for *Caenorhabditis elegans* with a blocked unfolded protein response. *J. Cell Biol.* **2002**, *158* (4), 639−646.

(56) Haskins, K. A.; Russell, J. F.; Gaddis, N.; Dressman, H. K.; Aballay, A. Unfolded protein response genes regulated by CED-1 are required for *Caenorhabditis elegans* innate immunity. *Dev. Cell* **2008**, *15* (1), 87−97.

(57) Styer, K. L.; Singh, V.; Macosko, E.; Steele, S. E.; Bargmann, C. I.; Aballay, A. Innate immunity in *Caenorhabditis elegans* is regulated by neurons expressing NPR-1/GPCR. *Science* **2008**, *322* (5900), 460−4.

(58) Lai, E.; Teodoro, T.; Volchuk, A. Endoplasmic reticulum stress: signaling the unfolded protein response. *Physiology* **2007**, *22* (3), 193−201.

(59) Viswanathan, M.; Kim, S. K.; Berdichevsky, A.; Guarente, L. A role for SIR-2.1 regulation of ER stress response genes in determining *C. elegans* life span. *Dev. Cell* **2005**, *9* (5), 605−615.

(60) Chung, S.; Gumienny, T. L.; Hengartner, M. O.; Driscoll, M. A common set of engulfment genes mediates removal of both apoptotic and necrotic cell corpses in *C. elegans*. *Nat. Cell Biol.* **2000**, *2* (12), 931−937.

(61) Reddien, P. W.; Horvitz, H. R. The engulfment process of programmed cell death in *Caenorhabditis elegans*. *Annu. Rev. Cell Dev. Biol.* **2004**, *20* (1), 193−221.

(62) Syntichaki, P.; Tavernarakis, N. The biochemistry of neuronal necrosis: rogue biology? *Nat. Rev. Neurosci.* **2003**, *4* (8), 672−684.

(63) Korswagen, H. C.; Park, J. H.; Ohshima, Y.; Plasterk, R. H. An activating mutation in a *Caenorhabditis elegans* Gs protein induces neural degeneration. *Genes Dev.* **1997**, *11* (12), 1493−1503.

(64) Shen, X.; Ellis, R. E.; Sakaki, K.; Kaufman, R. J. Genetic interactions due to constitutive and inducible gene regulation mediated by the unfolded protein response in *C. elegans*. *PLoS Genet.* **2005**, *1* (3), e37.

(65) Zhou, Z.; Hartwieg, E.; Horvitz, H. R. CED-1 is a transmembrane receptor that mediates cell corpse engulfment in *C. elegans*. *Cell* **2001**, *104* (1), 43−56.

(66) He, B.; Yu, X.; Margolis, M.; Liu, X.; Leng, X.; Etzion, Y.; Zheng, F.; Lu, N.; Quiocho, F. A.; Danino, D.; Zhou, Z. Live-cell imaging in *Caenorhabditis elegans* reveals the distinct roles of dynamin self-assembly and guanosine triphosphate hydrolysis in the removal of apoptotic cells. *Mol. Biol. Cell* **2010**, *21* (4), 610−629.

(67) Yu, X.; Odera, S.; Chuang, C.-H.; Lu, N.; Zhou, Z. *C. elegans* dynamin mediates the signaling of phagocytic receptor CED-1 for the engulfment and degradation of apoptotic cells. *Dev. Cell* **2006**, *10* (6), 743−757.

(68) Yu, X.; Lu, N.; Zhou, Z. Phagocytic receptor CED-1 initiates a signaling pathway for degrading engulfed apoptotic cells. *PLoS Biol.* **2008**, *6* (3), No. e61.